2864 © *1993 The Chemical Society of Japan* *Bull. Chem. Soc. Jpn.,* ***66****, 2864—2870(1993)* [Vol. 66, No. 10

Ion-Molecule Reactions of CO_2^+ with Butane and Isobutane at Thermal Energy

Masaharu TSUJI,*[†,††] Ken-ichi MATSUMURA,[††] Tsuyoshi FUNATSU,[††] Yukio NISHIMURA,[†,††] Hiroshi OBASE,[†††]
Shinji KAGAWA,[†††] and Yasuhito KANETAKA[†††]
† Institute of Advanced Material Study, Kyushu University, Kasuga, Fukuoka 816
†† Department of Molecular Science and Technology, Graduate School of Engineering Sciences, Kyushu University, Kasuga, Fukuoka 816
††† Department of Industrial Chemistry, Faculty of Engineering, Tohwa University, Minami-ku, Fukuoka 815

(Received May 26, 1993)

Rate constants and product ion distributions have been determined for thermal energy reactions of CO_2^+ with n-C_4H_{10} and i-C_4H_{10} by using an ion-beam apparatus. The total rate constants are $(9.8\pm2.0)\times10^{-10}$ and $(1.0\pm0.2)\times10^{-9}$ cm^3 s^{-1} for n-C_4H_{10} and i-C_4H_{10}, respectively. These values amount to about 75% of the collision rate constants estimated from the Langevin theory. $C_4H_9^+$, $C_3H_n^+$ (n=5—7), and $C_2H_n^+$ (n=3—5) are produced from n-C_4H_{10} with branching ratios of 6, 56, and 38%, while $C_4H_9^+$ and $C_3H_n^+$ (n=5—7) are formed from i-C_4H_{10} with branching ratios of 7 and 93%, respectively. The lack of $C_2H_n^+$ fragments from i-C_4H_{10} is attributed to a low probability of significant rearrangement of chemical bonds for the formation of the $C_2H_n^+$ fragments. The product ion distribution in the CO_2^+/n-C_4H_{10} reaction is in good agreement with that predicted from the fragmentation pattern of n-$C_4H_{10}^+$ at 13.78 eV, indicating that the CO_2^+/n-C_4H_{10} reaction proceeds through a near-resonant charge transfer without momentum transfer.

We have recently developed a new type of ion-beam apparatus for studying ion-molecule reactions at thermal energy.[1,2)] A flowing-afterglow apparatus was used as a reactant ion source. One advantage of our beam apparatus is that the reactant ion is completely thermalized at room temperature in the ion source before entering the reaction zone. The other one is that the operating pressure is much lower than those in the conventional flowing-afterglow and selected-ion-flow-tube (SIFT) methods used for studying thermal ion-molecule reactions. Therefore, more reliable kinetic data can be obtained without influence of secondary collisions with the buffer gas. More recently, our beam apparatus has been successfully applied to the study of charge-transfer (CT) reactions of Ar^+ with n-C_4H_{10} and i-C_4H_{10} at thermal energy.[3)] The total reaction rate constants were determined to be $(7.9\pm2.8)\times10^{-10}$ cm^3 s^{-1} and $(8.6\pm3.1)\times10^{-10}$ cm^3 s^{-1} for n-C_4H_{10} and i-C_4H_{10}, respectively. These values amount to about 60% of calculated values from the Langevin theory. Major product ions were $C_2H_5^+$ (36%), $C_2H_3^+$ (32%), and $C_3H_5^+$ (22%) for n-C_4H_{10}, while $C_2H_3^+$ (46%) and $C_3H_5^+$ (42%) for i-C_4H_{10}. A comparison of the observed product ion distribution with a reported breakdown scheme of n-$C_4H_{10}^+$ indicated that the Ar^+/n-C_4H_{10} reaction occurs through near-resonant CT.

Since the discovery of a large amount of the CO_2^+ ion in the Martian and Venus atmospheres,[4,5)] there has been continuous interest in ion-molecule reactions of CO_2^+ with simple molecules.[6,7)] We study here thermal CT reactions of CO_2^+ with n-C_4H_{10} and i-C_4H_{10} by using the thermal ion-beam apparatus. The rate constants and product ion distributions are determined. The CT process of CO_2^+/n-C_4H_{10} is discussed by reference to reported breakdown curves of the parent cation. The results obtained are compared with those for the Ar^+/C_4H_{10} reactions to obtain information on the difference in reactivity between the molecular ion and the atomic one.

Experimental

The thermal ion-beam apparatus used in the present study was similar to that used for the Ar^+/C_4H_{10} reactions[3)] except for the addition of a CO_2 inlet in a reactant ion source. In brief, a mixture of the ground-state $Ar^+(^2P_{3/2,1/2})$ ions, high energy metastable $(Ar^+)^*$ ions, and the metastable $Ar(^3P_{2,0})$ atoms were generated by a microwave discharge of high purity Ar gas in a quartz flow tube.[8)] The metastable $(Ar^+)^*$ ions were more rapidly quenched than $Ar^+(^2P_{3/2,1/2})$ while flowing in a quartz tube. Therefore, a long distance of about 30—40 cm between the microwave discharge and the CO_2 gas inlet was used to isolate $Ar^+(^2P_{3/2,1/2})$. There are two spin-orbit states, $Ar^+(^2P_{3/2})$ and $Ar^+(^2P_{1/2})$, with recombination energies of 15.76 and 15.92 eV, respectively. The lack of the upper $Ar^+(^2P_{1/2})$ component in the Ar flowing afterglow was confirmed by observing ArF(B-X,D-X) excimers resulting from the spin-orbit state selective $Ar^+(^2P_{3/2,1/2})/SF_6^-$ ionic-recombination reaction.[9,10)] The metastable $Ar(^3P_{2,0})$ atoms were completely quenched by the addition of CO_2. The $CO_2^+(\tilde{X})$ ions were produced by the thermal energy CT reaction of Ar^+ with CO_2:

$$Ar^+(^2P_{3/2}) + CO_2 \xrightarrow{k_1} CO_2^+(\tilde{X}) + Ar, \quad (1)$$
$$k_1 = (5.6 \pm 1.3) \times 10^{-10} \text{ cm}^3\,\text{s}^{-1}.^{11,12)}$$

After being completely thermalized by collisions with the buffer Ar gas, CO_2^+ ions were expanded into a low pressure chamber through a molybdenum nozzle centered on the flow tube. The vibrational frequency of ν_1 mode in $CO_2^+(\tilde{X})$ is 1280 cm^{-1},[13)] and hence less than 0.2% of $CO_2^+(\tilde{X})$ would be populated in the vibrational excited state at 300 K. It is therefore expected that the contribution of vibrationally excited $CO_2^+(\tilde{X})$ was negligibly small under the present experimental condition.

The sample gas was kept at a constant mass flow and injected from a stainless steel orifice placed 5 cm downstream from the nozzle. The reactant and product ions were sampled through a molybdenum orifice placed 3 cm further downstream and analyzed using a quadrupole mass spectrometer. The mass spectra were averaged using a digital storage oscilloscope and stored in a microcomputer. Operating pressures were (0.5—0.7) Torr (1 Torr=133.3 Pa) in the ion-source chamber, $(2.0—4.0)\times10^{-3}$ Torr in the reaction chamber, and $(0.8—2.4)\times10^{-5}$ Torr in the mass analyzing chamber.

Results and Discussion

Rate Constants. Figure 1 shows semilogarithmic plots of CO_2^+ ion current vs. a reagent flow rate. Total rate constants $k_{C_4H_{10}}$ are determined from the decay of CO_2^+, which is governed by the pseudo-first-order rate law,

$$I(CO_2^+) = I_0(CO_2^+)\exp(-k_{C_4H_{10}}[C_4H_{10}]t). \quad (2)$$

Here, $I_0(CO_2^+)$ represents the initial CO_2^+ ion current and t is the reaction time. Because of the difficulty in evaluating the accurate t value, the $k_{C_4H_{10}}$ values are evaluated with reference to the rate constant of the CO_2^+/CH_4 reaction (k_{CH_4}), which has been well established as $(1.0\pm0.1)\times10^{-10}$ $cm^3\,s^{-1}$,[11]

$$k_{C_4H_{10}} = k_{CH_4}\frac{\ln\{I(CO_2^+)/I_0(CO_2^+)\}_{C_4H_{10}}}{\ln\{I(CO_2^+)/I_0(CO_2^+)\}_{CH_4}}\frac{[CH_4]}{[C_4H_{10}]}. \quad (3)$$

The decay of CO_2^+ with the addition of CH_4 under the same experimental conditions is also shown in Fig. 1. The rate constants obtained from slopes in Fig. 1 are summarized in Table 1. The accuracies of the present kinetic data are estimated by summing up an experimental error of $k_{C_4H_{10}}$ and uncertainties of the reported k_{CH_4} values (±10%). In Table 1 are also given the calculated collision rate constants from the Langevin theory,[14]

$$k_{\mathrm{calcd}} = 2\pi e(\alpha/\mu)^{1/2}, \quad (4)$$

where α and μ are polarizability of C_4H_{10}[15] and a reduced mass of the reactant system, respectively. The observed $k_{C_4H_{10}}$ values amount to 75—77% of the calculated values.

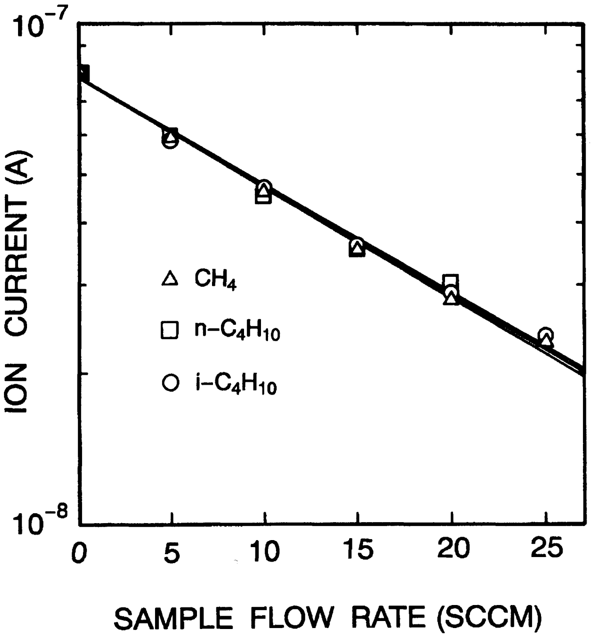

Fig. 1. The variation of the reactant ion current with the sample gas flow for the $CO_2^+/n\text{-}C_4H_{10}$ and $CO_2^+/i\text{-}C_4H_{10}$ reactions. As a reference the decay of CO_2^+ with the addition of CH_4 under the same experimental conditions is shown.

Table 1. Observed and Calculated Reaction Rate Constants of the CO_2^+/C_4H_{10} Reactions at Thermal Energy

Reactions	k_{obsd}	k_{calcd} a)	$k_{\mathrm{obsd}}/k_{\mathrm{calcd}}$
	10^{-9} $cm^3\,s^{-1}$		
$CO_2^+ + n\text{-}C_4H_{10}$	0.98±0.20	1.3	0.75±0.15
$CO_2^+ + i\text{-}C_4H_{10}$	1.0±0.2	1.3	0.77±0.15

a) Calculated from Langevin theory.

According to an ion cyclotron resonance (ICR) study by Laudenslager et al.,[16,17] the thermal CT reactions of rare gas ions with simple molecules are fast when there is an energy resonant state with favorable Franck–Condon factors (FCFs) for ionization. On the other hand, valid information about the importance of FCFs could not be obtained from the rate constants of the reactions of molecular O_2^+, N_2^+, CO^+, and CO_2^+ ions with CH_4 in an ICR study of Ausloos et al.[18] In order to determine the relative importance of the FCFs in the present systems, the reported photoelectron spectra (PES) of n-C_4H_{10} and i-C_4H_{10} are compared with the recombination energy of the reactant CO_2^+ ion (13.78 eV) in Fig. 2. Energy resonant states with favorable FCFs are present for both molecules. On the basis of the SIFT study of Rakshit and Warneck[6] and our recent beam study,[20] the reaction rate constant for the CO_2^+/C_2H_2 reaction is also large (5.6 or 7.3×10^{-10} $cm^3\,s^{-1}$), even though resonant state is absent. These values correspond to 51 or 66% of the k_{calcd} values. It may therefore be reasonable to assume that the existence of favorable FCFs is not the appropriate criterion for assessing the magnitude of the thermal CT reactions of CO_2^+ with hydrocarbons. Our finding is consistent with that of Ausloos et al.[18]

Product Ion Distributions. Typical mass spectra obtained in the $CO_2^+/n\text{-}C_4H_{10}$ and $CO_2^+/i\text{-}C_4H_{10}$ reactions are shown in Figs. 3(a) and 3(b), respectively. In both spectra, $C_3H_n^+$ (n=5—7) and $C_4H_9^+$ are found. In addition, $C_2H_n^+$ (n=3—5) are detected at low mass numbers in the $CO_2^+/n\text{-}C_4H_{10}$ spectrum. Although CO_2H^+ ion resulting from hydrogen atom transfer has been obtained for the CO_2^+/CH_4 reaction as a major product,[6,7,20] it could not be detected in the $CO_2^+/n\text{-}C_4H_{10}$ and $CO_2^+/i\text{-}C_4H_{10}$ reactions. Some primary product ions further react with reagent C_4H_{10} gas to yield secondary ions at high gas flow rates. In order

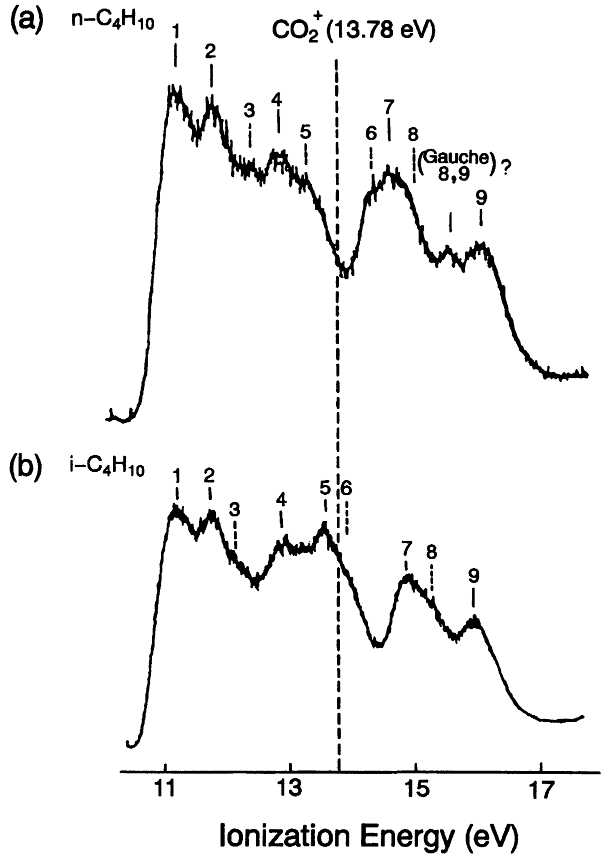

Fig. 2. Photoelectron spectra of n-C_4H_{10} and i-C_4H_{10}. The broken line indicates the recombination energy of CO_2^+. Adopted from Ref. 19. n-C_4H_{10}: Peak 1 (IP_v=11.09 eV, 14a′, σ_{CC}), 2 (11.66 eV, 3a″, π_{CH_2}), 3 (12.3 eV, 13a′, σ_{CC}), 4 (12.74 eV, 2a″, π_{CH_3}), 5 (13.2 eV, 12a′, σ_{CC}), 6 (14.2 eV, 1a″, π_{CH_3}), 7 (14.59 eV, 11a′, π_{CH_3}), 8 (15.0 eV, 10a′, σ_{CC}), and 9 (15.99 eV, 9a′, π_{CH_2}), and i-C_4H_{10}: Peak 1 (IP_v=11.13 eV, 6a$_1$, $\sigma_{CH}+\sigma_{CC}$), 2 (11.70 eV, 5e, σ_{CC}), 3 (12.1 eV, 5e, σ_{CC}), 4 (12.85 eV, 1a$_2$, π_{CH_3}), 5 (13.52 eV, 4e, π_{CH_3}), 6 (13.9 eV, 4e, π_{CH_3}), 7 (14.86 eV, 3e, π_{CH_3}), 8 (15.3 eV, 3e, π_{CH_3}), and 9 (15.95 eV, 5a$_1$, π_{CH_3}).

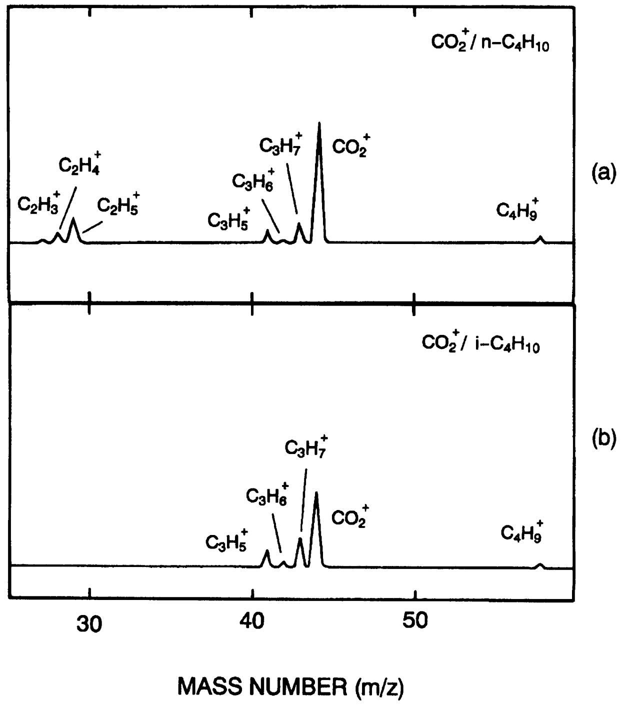

Fig. 3. Typical mass spectra resulting from the (a) CO_2^+/n-C_4H_{10} and (b) CO_2^+/i-C_4H_{10} reactions at thermal energy. The spectra are uncorrected for the relative sensitivity.

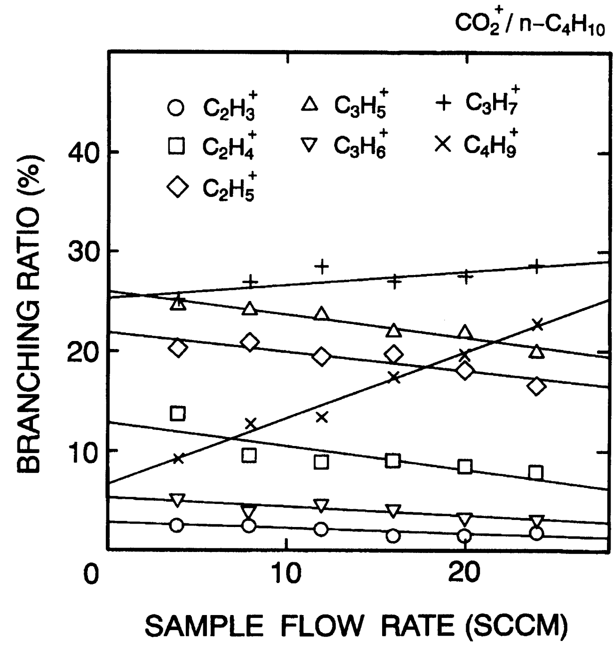

Fig. 4. The variation of the branching fractions of the ionic products with n-C_4H_{10} flow for the CO_2^+/n-C_4H_{10} reaction.

to determine the contribution of such secondary reactions, the dependence of branching ratios of each product ion on the C_4H_{10} flow rate is measured, as shown in Figs. 4 and 5. With increasing the n-C_4H_{10} flow rate, the branching ratios of $C_3H_7^+$ and $C_4H_9^+$ increase, while those of $C_3H_5^+$, $C_2H_5^+$, $C_2H_4^+$, $C_3H_6^+$, and $C_2H_3^+$ decrease. This indicates that the secondary reactions of the latter ions with n-C_4H_{10} take part in the formation of the former ions. With increasing the i-C_4H_{10} flow rate, the branching ratios of $C_3H_5^+$ and $C_4H_9^+$ decreases and increases, respectively, indicating that the $C_3H_5^+$/i-C_4H_{10} reaction participates in the formation of $C_4H_9^+$. The branching ratios of $C_3H_7^+$ and $C_4H_6^+$ are essentially independent of the i-C_4H_{10} flow rate. Combining above findings and the known reactions of the hydrocarbon system,[11] the reaction scheme of the CO_2^+/n-C_4H_{10} and CO_2^+/i-C_4H_{10} CT is summarized as follows:

$$CO_2^+ + n\text{-}C_4H_{10} \longrightarrow C_4H_9^+ + H + CO_2, \qquad (5a)$$

$$\longrightarrow C_3H_7^+ + CH_3 + CO_2, \qquad (5b)$$

$$\longrightarrow C_3H_6^+ + CH_4 + CO_2, \qquad (5c)$$

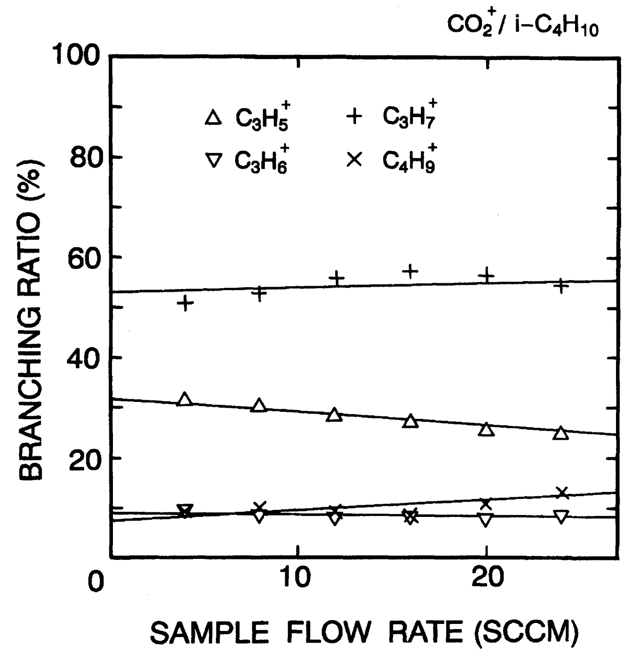

Fig. 5. The variation of the branching fractions of the ionic products with *i*-C_4H_{10} flow for the CO_2^+/i-C_4H_{10} reaction.

$$\longrightarrow C_3H_5^+ + (CH_4 + H, CH_3 + H_2) + CO_2, \quad (5d)$$

$$\longrightarrow C_2H_5^+ + (C_2H_5, C_2H_4 + H) + CO_2, \quad (5e)$$

$$\longrightarrow C_2H_4^+ + C_2H_6 + CO_2, \quad (5f)$$

$$\longrightarrow C_2H_3^+ + CH_4 + CH_3 + CO_2. \quad (5g)$$

$$C_2H_3^+ + n\text{-}C_4H_{10} \longrightarrow C_3H_7^+ + C_3H_6 + 1.14 \text{ eV}. \quad (6)$$

$$C_2H_4^+ + n\text{-}C_4H_{10} \longrightarrow C_4H_9^+ + C_2H_5 + 0.02 \text{ eV}, \quad (7a)$$

$$\longrightarrow C_3H_7^+ + C_3H_7 - 0.06 \text{ eV}. \quad (7b)$$

$$C_2H_5^+ + n\text{-}C_4H_{10} \longrightarrow C_4H_9^+ + C_2H_6 + 0.22 \text{ eV}. \quad (8)$$

$$C_3H_5^+ + n\text{-}C_4H_{10} \longrightarrow C_4H_9^+ + C_3H_6 - 0.41 \text{ eV}. \quad (9)$$

$$CO_2^+ + i\text{-}C_4H_{10} \longrightarrow C_4H_9^+ + H + CO_2, \quad (10a)$$

$$\longrightarrow C_3H_7^+ + CH_3 + CO_2, \quad (10b)$$

$$\longrightarrow C_3H_6^+ + CH_4 + CO_2, \quad (10c)$$

$$\longrightarrow C_3H_5^+ + (CH_4 + H, CH_3 + H_2) + CO_2. \quad (10d)$$

$$C_3H_5^+ + i\text{-}C_4H_{10} \longrightarrow C_4H_9^+ + C_3H_6 - 0.41 \text{ eV}. \quad (11)$$

Here, the ΔH values are calculated from reported thermochemical data.[21] Processes (7b), (9), and (11) are endoergic. The reactant $C_2H_4^+$ and $C_3H_5^+$ ions produced in primary reactions (5d), (5f), and (10d) are expected to maintain some internal and/or kinetic energies because of low operating pressures. Thus, these endoergic secondary reactions become possible under the present experiment. The rate constants of processes (6), (7), (8), (9), and (11) have been estimated to be $(8.5\pm1.0)\times10^{-10}$, $(1.14\pm0.13)\times10^{-9}$, $(8.4\pm0.2)\times10^{-10}$, $(5.0\pm0.6)\times10^{-10}$, and $(5.8\pm0.4)\times10^{-10}$ $cm^3 s^{-1}$, respectively, though the product ions have not been identified.[11]

By extrapolating the percentages of each product ion to zero C_4H_{10} flow, the initial branching ratios in primary reactions (5) and (10) are determined. The results obtained are given in Table 2. The $C_2H_n^+$ (n=3—5), $C_3H_n^+$ (n=5—7), and $C_4H_9^+$ fragments occupy 38, 56, and 6% of the total product ions for n-C_4H_{10}, respectively. On the other hand, the $C_3H_n^+$ (n=5—7) and $C_4H_9^+$ fragments occupy 93 and 7% of the total product ions for i-C_4H_{10}, respectively. It should be noted that $C_2H_n^+$ fragments are absent for i-C_4H_{10}. The $C_2H_n^+$ fragments can be easily formed from n-$C_4H_{10}^+$ by cleavage of C–C and C–H bonds without significant rearrangement of chemical bonds. Meanwhile, cleavage of two skeletal C–C bonds followed by creation of a new C–C bond is required for the formation of the $C_2H_n^+$ fragments from i-$C_4H_{10}^+$. Thus, the lack of the $C_2H_n^+$ fragments in i-C_4H_{10} can be attributed to a low probability of significant rearrangement of chemical bonds in the dissociation of i-$C_4H_{10}^+$.

Charge-Transfer Mechanism. The appearance potentials of each product ion are shown in Table 2. In the CT reactions of CO_2^+ with n-C_4H_{10} and i-C_4H_{10}, fragment ions with appearance potentials of 10.93—14.55 eV are observed. All of these energies are lower than the recombination energy of CO_2^+ (13.78 eV) except for the appearance potential of $C_3H_5^+$ from i-$C_4H_{10}^+$, which has been measured as 14.55 eV under electron-impact ionization.[22] The present observation of $C_3H_5^+$ from i-C_4H_{10} suggests that the appearance potential of $C_3H_5^+$ from i-C_4H_{10} in the thermal CT reaction must be lower than 13.78 eV. In general, molecular ions are produced via vertical ionization under high energy electron-impact ionization, where FCFs for ionization dominate the reaction. Therefore, an excess energy over the dissociation limit is often necessary for the formation of a precursor ionic state with favorable FCFs. On the other hand, energy-resonance requirement generally takes precedence over FCFs for ionization in the thermal CT reaction. Thus, the ionization into a lower precursor state with poor FCFs becomes possible.

Figure 6 shows breakdown curves of n-$C_4H_{10}^+$ obtained by Chupka and Lindholm using various atomic and molecular ion beams with collisional energies of 5 and 900 eV.[23] For comparison, the product ion distribution obtained in the thermal CO_2^+/n-C_4H_{10} is also given in Fig. 6 at 13.78 eV. It should be noted that a good agreement is found between the observed distribution and the breakdown curves at 13.78 eV. Assuming that the breakdown curves obtained by the ion-beam method gives exact fragmentation pattern of n-$C_4H_{10}^+$, this finding leads us to conclude that the CO_2^+/n-C_4H_{10} reaction proceeds through near-resonant CT. Combining this result with the relatively large reaction rate

Table 2. Product Ion Distributions in the CO_2^+/C_4H_{10} Reactions, Photoionization, and Electron-Impact Ionization of C_4H_{10}

Reactant molecule	Product ion	Appearance potential (eV)[a]	Branching ratio (%)		
			CO_2^+	Photoionization	Electron impact
			13.78 eV	14.0 eV	70 eV
			This work[b]	Ref. 24	Ref. 25
n-C_4H_{10}	$C_4H_{10}^+$	10.55	0	10.80	4
	$C_4H_9^+$	11.65	6	1.64	0
	$C_4H_7^+$	12.51	0	0	0
	$C_3H_7^+$	11.19	25	52.75	35
	$C_3H_6^+$	11.16	5	6.61	4
	$C_3H_5^+$	13.40	26	5.87	10
	$C_3H_3^+$	14.96	0	0	4
	$C_2H_5^+$	12.55	22	10.20	15
	$C_2H_4^+$	11.65	13	10.39	11
	$C_2H_3^+$	13.66	3	1.07	13
	$C_2H_2^+$	13.52	0	0	2
	CH_3^+	13.35	0	0	2
	Other ions		0	0.68	0
i-C_4H_{10}	$C_4H_{10}^+$	10.57	0		0
	$C_4H_9^+$	11.60	7		1
	$C_3H_8^+$	15.33	0		1
	$C_3H_7^+$	11.23	53		42
	$C_3H_6^+$	10.93	9		14
	$C_3H_5^+$	14.55	31		16
	$C_3H_3^+$	15.05	0		7
	$C_3H_2^+$		0		1
	$C_2H_5^+$	13.80	0		3
	$C_2H_4^+$	11.65	0		0
	$C_2H_3^+$	13.75	0		12
	CH_3^+	14.75	0		3

a) Ref. 21. b) Uncertainties ±7%.

constant described before, it can be concluded that the electron jump occurs at long range without momentum transfer in this reaction system. We have recently found that the Ar^+/n-C_4H_{10} reaction proceeds through a similar near-resonant process in which the breakdown of precursor n-$C_4H_{10}^{+*}$ ion occurs near the recombination energy of $Ar^+(^2P_{3/2}$: 15.76 eV). Although internal degrees of freedom in n-$C_4H_{10}^{+*}$ and translational degrees of freedom in products are acceptable modes of excess energy in the Ar^+ reaction, internal (vibrational and rotational) degrees of freedom in CO_2 become additional acceptable modes in the CO_2^+ reaction:

$$Ar^+ + n\text{-}C_4H_{10} \longrightarrow n\text{-}C_4H_{10}^{+*} + Ar + \Delta E_{ex}, \tag{12a}$$

$$\begin{aligned}\Delta E_{ex} &= RE(Ar^+) - IP_a(n\text{-}C_4H_{10}) \\ &= E_{int}(n\text{-}C_4H_{10}^{+*}) + E_{trans}(Ar, n\text{-}C_4H_{10}^{+*}).\end{aligned} \tag{12b}$$

$$CO_2^+ + n\text{-}C_4H_{10} \longrightarrow n\text{-}C_4H_{10}^{+*} + CO_2 + \Delta E_{ex}, \tag{13a}$$

$$\begin{aligned}\Delta E_{ex} = RE(CO_2^+) - IP_a(n\text{-}C_4H_{10}) = E_{int}(n\text{-}C_4H_{10}^{+*}) \\ + E_{int}(CO_2) + E_{trans}(CO_2, n\text{-}C_4H_{10}^{+*}).\end{aligned} \tag{13b}$$

where RE and IP_a stand for the recombination energy and the adiabatic ionization potential, respectively. Thus, the possibility of non-resonant CT would be larger in the CO_2^+ reaction. However, the present result shows that process (13a) occurs almost resonantly. On the basis of this finding, the reactivity of molecular CO_2^+ ion is similar to that of atomic Ar^+ one in the CT reactions with n-C_4H_{10}, being independent of degrees of freedom of the reactant ion.

In order to compare the reactivity among the thermal CT, photoionization, and fast electron-impact ionization, the product ion distributions in photoionization at 14.0 eV and in electron-impact ionization at 70 eV are shown in Table 2. Prominent features in the ionization by photons and electrons for n-C_4H_{10} are a high branching fraction of $C_3H_7^+$ in comparison with those of $C_3H_5^+$ and $C_2H_5^+$ and the appearance of a small amount of the parent ion. Since the photoionization and the electron-impact ionization initially populate ionic states with favorable FCFs, the n-$C_4H_{10}^+$ states in the 11—13 eV region will be formed preferentially (see Fig. 2). According to the breakdown curves of n-$C_4H_{10}^+$, the parent $C_4H_{10}^+$ ion and the daughter $C_3H_7^+$ ion are major products in this energy region, which is in agreement with the experimental observation. Thus, the different prod-

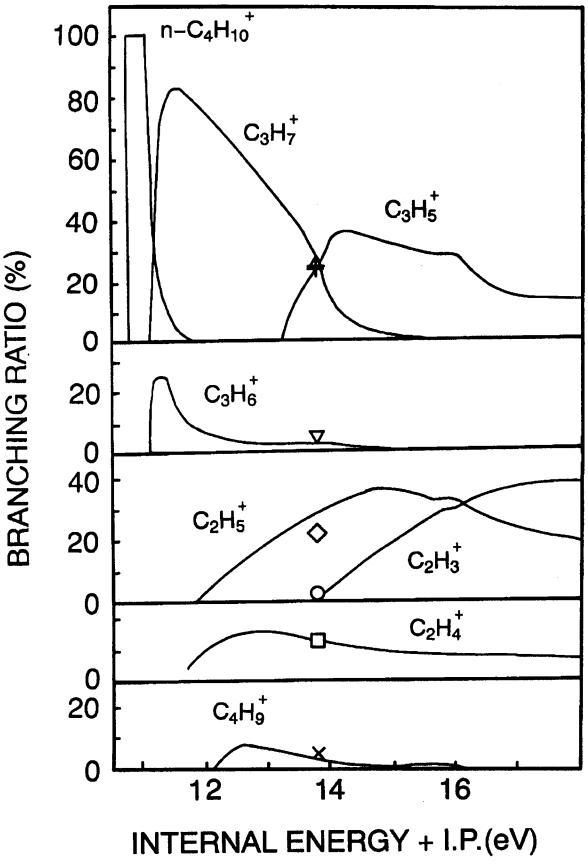

Fig. 6. Breakdown diagram of $n\text{-}C_4H_{10}^+$. Adopted from Ref. 23. Branching fractions in the $CO_2^+/n\text{-}C_4H_{10}$ reaction is shown at 13.78 eV.

uct ion distribution in the thermal CT reaction from those in the photoionization and the electron-impact ionization can be explained by the different ionization mechanism.

There are nine ionic states of $n\text{-}C_4H_{10}^+$ in the 11—17 eV region based upon PES shown in Fig. 2(a). In the caption of Fig. 2 are given vertical ionization potentials (IP_v) of each state, molecular orbitals of removed electrons, and their bonding characters reported by Kimura et al.[19] The $CO_2^+/n\text{-}C_4H_{10}$ reaction initially populates the parent $n\text{-}C_4H_{10}^+$ ion near 13.78 eV. Therefore, important precursor states are expected to be near-resonant states 5 and 6, arising loss of a 12a$'$ electron with σ_{CC} character and a 1a$''$ electron with π_{CH_3} character, respectively. The nature of molecular orbitals of the removed electrons suggests that the major $C_2H_n^+$ fragments dominantly arise from cleavage of a C–C bond in state 5(12a$'^{-1}$), while the minor $C_4H_9^+$ fragment arises from cleavage of a C–H bond in state 6(1a$''^{-1}$):

$$\begin{array}{l} CO_2^+ + n\text{-}C_4H_{10} \longrightarrow n\text{-}C_4H_{10}^+\ \text{(state 5)} + CO_2, \\ \qquad\qquad\qquad\qquad \downarrow \\ \qquad\qquad\qquad\qquad C_2H_n^+ (n = 3\text{—}5), \end{array} \tag{14a}$$

$$\begin{array}{l} \longrightarrow n\text{-}C_4H_{10}^+\ \text{(state 6)} + CO_2, \\ \qquad \downarrow \\ \qquad n\text{-}C_4H_9^+. \end{array} \tag{14b}$$

Similar ionic states are present for $i\text{-}C_4H_{10}$, as shown in Fig. 2(b). Ionization mechanism is uncertain for the $CO_2^+/i\text{-}C_4H_{10}$ reaction because of the lack of breakdown curve. However, it may be reasonable to assume that the reaction also proceeds through near-resonant CT. Possible near-resonant precursor states of $i\text{-}C_4H_{10}^+$ are states 5 and 6, arising from loss of a 4e electron with π_{CH_3} character. Therefore, the major $C_3H_n^+$ ions are probably formed through cleavage of a C–H bond followed by a C–C bond dissociation.

Summary

Thermal energy reactions of CO_2^+ with $n\text{-}C_4H_{10}$ and $i\text{-}C_4H_{10}$ have been investigated by using an ion-beam apparatus. The rate constants and product distributions were determined and summarized in Tables 1 and 2, respectively. The total rate constants correspond to about 75% of the collision rate constants estimated from the Langevin theory. For all reactions, only CT product channels were observed and no evidence of hydrogen atom transfer channels was found. The product ion distribution led us to conclude that near-resonant CT occurs in the $CO_2^+/n\text{-}C_4H_{10}$ reaction.

We wish to express their thanks to Professor C.E. Brion of Univ. British Columbia for his sending a preprint of Ref. 24. This work was supported by a Grant-in-Aid for Developmental Scientific Research No. 02555170 from the Ministry of Education, Science, and Culture, the Asahi Glass Foundation, the Ito Science Foundation, and the Morino Foundation for molecular science.

References

1) M. Tsuji, F. Funatsu, H. Kouno, Y. Nishimura, and H. Obase, *J. Chem. Phys.*, **96**, 3649 (1992).

2) M. Tsuji, H. Kouno, K. Matsumura, T. Funatsu, Y. Nishimura, H. Obase, H. Kugishima, and K. Yoshida, *J. Chem. Phys.*, **98**, 2011 (1993).

3) M. Tsuji, K. Matsumura, T. Funatsu, H. Kouno, Y. Nishmura, H. Obase, S. Kagawa, Y. Kanetaka, H. Kugishima, and K. Yoshida, *J. Mass Spectrom. Soc. Jpn.*, **41**, 63 (1993).

4) M. B. McElroy, *J. Geophys. Res.*, **73**, 1513 (1968).

5) A. I. Stewart, *J. Geophys. Res.*, **77**, 54 (1972).

6) A. B. Rakshit and P. Warneck, *J. Chem. Soc., Faraday Trans. 2*, **76**, 1084 (1980).

7) N. W. Copp, M. Hamdan, J. D. C. Jones, K. Birkinshaw, and N. D. Twiddy, *Chem. Phys. Lett.*, **88**, 508 (1982).

8) M. Tsuji, in "Techniques of Chemistry," ed by J. M. Farrar and W. H. Saunders, Jr., John Wiley & Sons, New York (1988), Vol. 20, Chap. 9, pp. 489—562.

9) M. Tsuji, M. Furusawa, and Y. Nishimura, *J. Chem. Phys.*, **92**, 6502 (1990).

10) M. Tsuji, M. Ide, T. Muraoka, and Y. Nishimura, *J. Chem. Phys.*, **99**, 1710 (1993).

11) Y. Ikezoe, S. Matsuoka, M. Takebe, and A. Viggiano, "Gas-Phase Ion-Molecule Reaction Rate Constants through 1986," Maruzen, Tokyo (1987), and references therein.

12) R. J. Shul, B. L. Upschulte, R. Passarella, R. G. Keesee, and A. W. Castleman, Jr., *J. Phys. Chem.*, **91**, 2556 (1987).

13) G. Herzberg, "Electronic Spectra and Electronic Structure of Polyatomic Molecules," Van Nostrand Reinhold, New York (1966), p. 594.

14) G. Gioumousis and D. P. Stevenson, *J. Chem. Phys.*, **29**, 294 (1958).

15) "CRC Handbook of Chemistry and Physics," 68th ed, ed by R. C. Weast, M. J. Astle, and W. H. Beyer, CRC Press, Florida (1987—1988).

16) J. B. Laudenslager, W. T. Huntress, Jr., and M. T. Bowers, *J. Chem. Phys.*, **61**, 4600 (1974).

17) V. G. Anicich, J. B. Laudenslager, W. T. Huntress, Jr., and J. H. Futrell, *J. Chem. Phys.*, **67**, 4340 (1977).

18) P. Ausloos, J. R. Eyler, and S. G. Lias, *Chem. Phys. Lett.*, **30**, 21 (1975).

19) K. Kimura, S. Katsumata, Y. Achiba, T. Yamazaki, and S. Iwata, "Handbook of HeI Photoelectron Spectra of Fundamental Organic Molecules," Japan Sci. Soc. Press, Tokyo (1981).

20) M. Tsuji, K. Matsumura, T. Funatsu, Y. Nishimura, and H. Obase, *J. Chem. Phys.*, submitted for publication.

21) H. M. Rosenstock, K. Draxl, B. W. Steiner, and J. T. Herron, *J. Phys. Chem. Ref. Data*, **6**, Suppl. 1 (1977).

22) I. Omura, *Bull. Chem. Soc. Jpn.*, **34**, 1227 (1961).

23) W. A. Chupka and E. Lindholm, *Ark. Fys.*, **25**, 349 (1963).

24) J. W. Au, G. Cooper, and C. E. Brion, *Chem. Phys.*, **173**, 241 (1993).

25) A. Cornu and R. Massot, "Compilation of Mass Spectral Data," Heiden, London (1966).